ISSN 1028-3358, Doklady Physics, 2023, Vol. 68, No. 10, pp. 349–353. © Pleiades Publishing, Ltd., 2023.
Russian Text © The Author(s), 2023, published in Doklady Rossiiskoi Akademii Nauk. Fizika, Tekhnicheskie Nauki, 2023, Vol. 512, pp. 73–77.

TECHNICAL SCIENCE

The Significance of Retained Austenite in the High Strength and Plasticity of Medium Carbon Q&P Steel

R. V. Mishnev[a,b,*], Yu. I. Borisova[a,b], Academician M. N. Erokhin[a], S. M. Gaidar[a], and R. O. Kaibyshev[a]

Received March 16, 2023; revised March 16, 2023; accepted May 10, 2023

Abstract—The Fe–0.44%C–1.8%Si–1.3%Mn–0.82%Cr–0.28%Mo steel treated by the quenching–partitioning process showed a product of strength and elongation of 30 GPa % with yield stress of 1350 MPa. Such a combination of high ultimate tensile strength and good ductility is attributed to a high portion of retained austenite (≥20%) transforming to martensite under tension. The high yield stress is provided by carbon supersaturation of austenite and a high dislocation density in this phase.

Keywords: steel, mechanical properties, microstructure, phase transformation

DOI: 10.1134/S1028335823100063

The key characteristics of promising high-strength steels in advanced high strength steel (AHSS) are strength and ductility [1]. Materials can be strong or ductile, but the combination of high strength and good ductility is rare. A generally accepted criterion characterizing the combination of strength and ductility is the product of strength and elongation: $\sigma_B\delta$ (MPa %) [1, 2]. For third generation AHSS steels, the index $\sigma_B\delta$ should be from 20 to 40 GPa % [1]. Another requirement for these steels is the value of the yield strength ($\sigma_{0.2}$) ≥ 1000 MPa [1]. Combinations of such high $\sigma_{0.2}$ and $\sigma_B\delta$ were not achieved in steels of the first and second generation [1].

The contradiction between strength and ductility in steels can be overcome by heat treatment developed almost 20 years ago, which was called "Quenching and Partitioning," or Q&P [1–4]. This treatment involves heating above the temperature A_{c3}, complete austenitization followed by accelerated cooling in molten salt heated to a temperature T_q, between the start temperature (M_s) and end (M_{To}) martensitic transformation. Quenching in heated salt ensures the formation of primary martensite and retained austenite [1–5]. The next operation, "partitioning," is annealing, which is also usually carried out in molten salt heated to the temperature T_p, as a rule, above the temperature M_s; hence, $T_p > T_{Ms}$ [1–5]. During this operation, carbon is redistributed from primary martensite to retained austenite, which is enriched in carbon. At the same time, during "partitioning," a bainite transformation can occur, but the chemical composition of the steel and the temperature and time of partitioning are selected in such a way as to minimize the specific volume of the bainite being formed. It should be noted that the release of cementite is not allowed during the "partitioning" operation. This is achieved due to the high content (≥1.5 wt %) of Si in Q&P steels. The last operation in Q&P processing is quenching from the "partitioning" temperature, which leads to partial transformation of retained austenite into secondary martensite, which differs from primary martensite in its high carbon content.

Low-alloy steels for Q&P processing with a carbon content from 0.4 to 0.56% are characterized by a high value of the parameter $\sigma_B\delta \geq 30$ GPa %, which is two times or more higher than in low-alloy auto steels belonging to the first generation AHSS, in combination with $\sigma_{0.2} > 1000$ MPa. A feature of these steels is the presence in the structure of 12 to 30% retained austenite in the form of blocks after Q&P treatment [6–8]. The high ductility of these steels is associated with the TRIP effect (Transformation induced plasticity, plasticity induced by transformation) [9]. Under tension, almost 90% of the retained austenite transforms into martensite [10]. At the same time, the nature of the high yield strength in steels with a high content of retained austenite enriched in carbon after Q&P treatment is unclear and little studied. It is believed that retained austenite has a strength almost two times lower than the yield strength of Q&P steels [5], the high strength of which can be due to the summation of the strength of high-strength martensite and

[a] *Russian State Agrarian University, Moscow Timiryazev Agricultural Academy, Moscow, Russia*
[b] *Belgorod State University, Belgorod, Russia*
**e-mail: mishnev91@mail.ru*

low-strength austenite according to the additive law [1, 4].

The purpose of this study is to establish the reasons for the high value of the yield strength, relative elongation, and parameter $\sigma_B\delta$ in the new Fe-0.44%C steel after Q&P treatment.

The studies were carried out on steel Fe–0.44%C–1.81%Si–1.33%Mn–0.82%Cr–0.28%Mo (wt %), which was obtained by induction melting in air followed by electroslag remelting. Next, the steel was annealed at 1150°C for four hours, followed by forging. Samples with a thickness of 3 mm were subjected to a three-stage Q&P heat treatment, including austenitization at a temperature of 900°C for 5 min, followed by quenching in a salt bath heated to various temperatures T_q from 140 to 300°C with holding for 15 s and subsequent "partitioning" at the temperature T_p = 400°C for 60 s in a salt bath, followed by air cooling.

Tensile tests were carried out on samples with a working length of 35 mm and a cross section of 7 × 3 mm on an Instron 5882 testing machine at room temperature. Microstructural studies were carried out using a FEI Quanta 600 FEG scanning electron microscope equipped with an electron backscatter diffraction (EBSD) pattern analyzer. The dislocation density was determined from EBSD data using the method described in [11]. The volume fraction of retained austenite was calculated by X-ray diffraction (XRD) using a Rigaku Ultima IV diffractometer with a step size of 0.02 deg, 40 kV, and 40 mA.

The average carbon concentration in retained austenite was calculated using the formula given in [12]:

$$C_{CRA} = (a_\gamma - 3.547)/0.046, \quad (1)$$

where C_{CRA} is the carbon concentration in the retained austenite and a_γ is the austenite lattice parameter.

In tensile testing, the relative elongation varies from 17.5 to 21.4% in the quenching temperature range of 140–250°C, and the tensile strength varies from σ_B = 1780 MPa at T_q = 140°C to 1580 MPa at T_q = 250°C. As a result, at a quenching temperature ≤250°C, the value of $\sigma_B\delta$ is >30 GPa % (Fig. 1), which is two times higher than in auto steels belonging to the first generation AHSS [1]. The value $\sigma_{0.2}$ varies from 1370 MPa at T_q = 140°C to 1170 MPa at T_q = 250°C. There is no yield plateau observed on the σ–ε curves, and strain hardening begins after reaching the yield point and continues until necking is formed. Consequently, parts made of this steel can be produced by sheet stamping [1]. Increasing the quenching temperature from 260 to 300°C (M_s = 270°C) leads to a sharp decrease in plasticity and the parameter $\sigma_B\delta$, which is accompanied by a significant increase in both the yield strength and the tensile strength. The failure of a sample hardened at 300°C occurs with slight deformation after reaching the yield point.

Q&P treatment in the quenching temperature range of 140–250°C leads to the formation of a structure consisting of primary martensite, secondary martensite, and retained austenite (Fig. 2). Martensite has the typical morphology of lath martensite: initial austenite grains, blocks, packets, and laths [13]. Retained austenite grains have an irregular shape and are located between martensite blocks (Fig. 2). The average grain size of retained austenite is 2.65 μm (T_q = 200°C). It is important to note that the structure of steel after quenching is characterized by a high density of geometrically necessary dislocations, which characterizes the elastic bending of the lattice and is determined from EBSD pictures. In this case, the dislocation density in retained austenite ($\rho = 6.2 \times 10^{14}$ m^{-2}) and martensite are approximately the same at T_q = 200°C, which contradicts early ideas about the low dislocation density in retained austenite in Q&P steels [5].

The volume fraction of retained austenite increases from 16 to 25% with increasing T_q from 140 to 250°C (Fig. 3). A subsequent increase in the quenching temperature from 250 to 300°C leads to a decrease in the volume fraction of retained austenite to 5%. Thus, if primary martensite is not formed, then during "partitioning" there is no enrichment of retained austenite with carbon and it transforms into martensite when cooled from the temperature T_p. Reducing the content of retained austenite by five times with increasing the quenching temperature above M_s correlates with a decrease in plasticity and a decrease in the parameter $\sigma_B\delta$ by almost ten times, despite an increase in the tensile strength by more than 40%. It is obvious that the high plasticity and high values of $\sigma_B\delta$ of this steel, hardened at temperatures from 140 to 250°C, are associated with strain hardening during tension. The study of samples after tension in the fracture region (neck) using X-ray diffraction analysis showed that the volume fraction of retained austenite in the structure does not exceed 3%. Thus, more than 80% of the retained austenite is transformed into tensile deformation martensite, which provides tensile strain hardening, since the strength of martensite is higher than the strength of austenite at the same carbon content. This confirms the assumption that the high ductility of steel after Q&P treatment is associated with the TRIP effect.

To establish the nature of the high value of the yield strength of Fe-0.44%C type steel, it is necessary to estimate the yield strength ($\sigma_{0.2}$) of the retained austenite. This can be done based on the rule about the additive contribution of various hardening mechanisms to the overall yield strength for one structural component [14]:

$$\sigma_{0.2} = \sigma_0 + \sigma_{SS} + \sigma_{HP} + \sigma_{disl}, \quad (2)$$

where σ_0 is the lattice friction stress ~63.5 MPa in pure iron austenite [14, 15], σ_{SS} is the solid solution strengthening, σ_{HP} is the structural strengthening, and

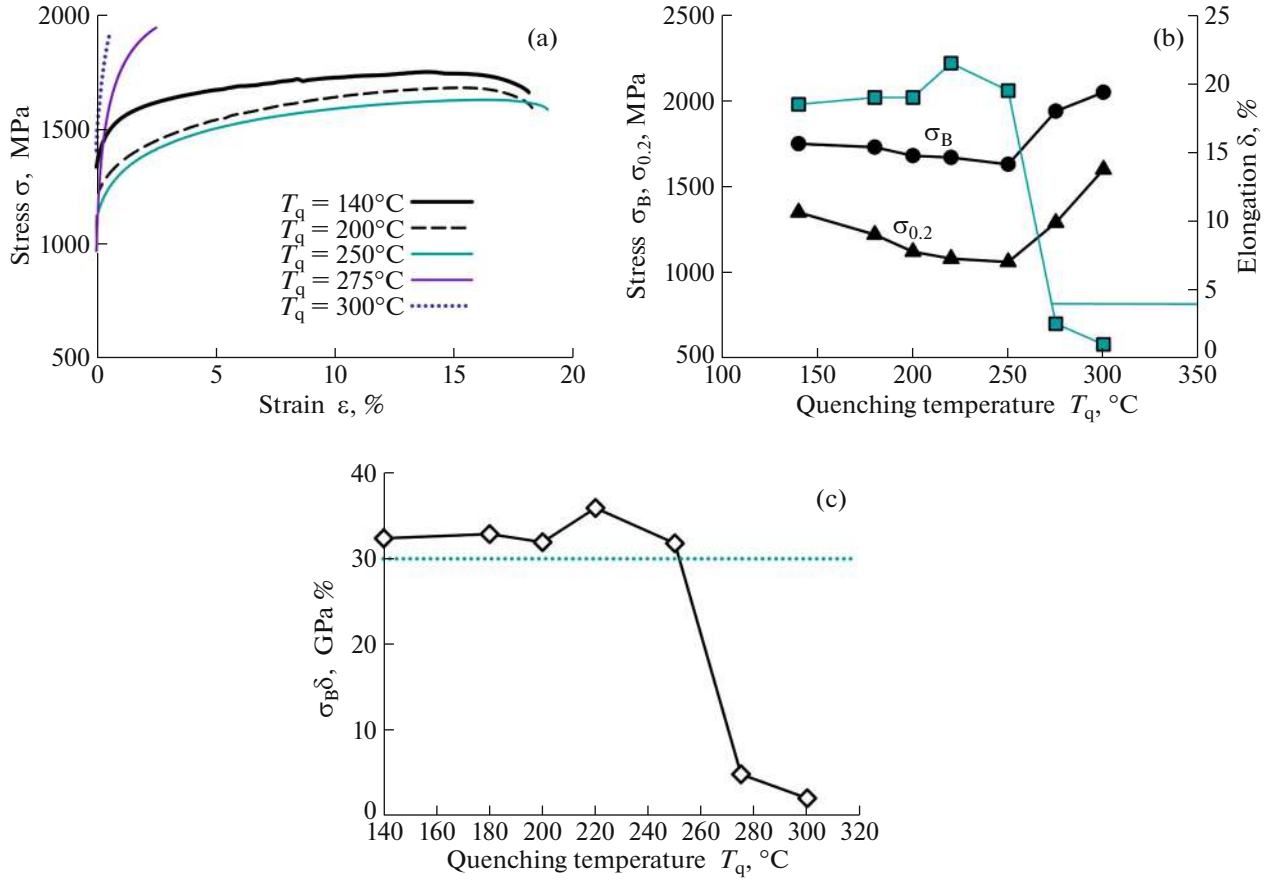

Fig. 1. (a) Engineering stress–strain curves, (b) the effect of quenching temperature on tensile mechanical properties (σ_B, $\sigma_{0.2}$, relative elongation), (c) dependence of the product of strength and elongation $\sigma_B\delta$ on the quenching temperature of the steel under study.

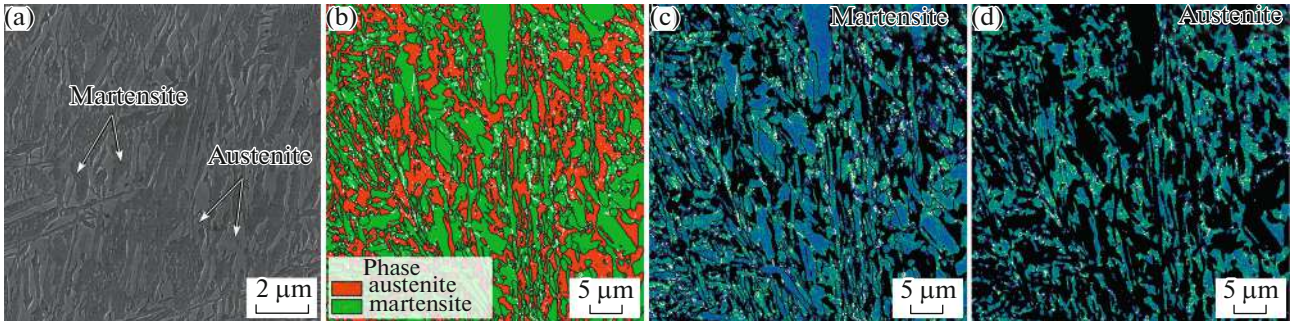

Fig. 2. Microstructure of Fe–0.44C steel after Q&P treatment at a quenching temperature of 200°C: (a) SEM and (b) EBSD analysis demonstrating the phase composition, (c) KAM picture for the martensitic phase, (d) KAM picture for the austenite phase (KAM is kernel average misorientations, elastic bending of the lattice).

σ_{disl} is the dislocation strengthening. Solid solution strengthening (σ_{SS}) is determined by the content of the elements of introduction and replacement and can be calculated using the following relation [14, 15]:

$$\sigma_{SS} = 356.5\times(\%C) + 20.1\times(\%Si) + 3.7\times(\%Cr) + 14.6\times(\%Mo). \quad (3)$$

The carbon concentration C_{CRA} = 1.38% was obtained by X-ray diffraction from Eq. (1), and the content of substitution elements in austenite was taken equal to the content in steel, since the redistribution between structural components does not occur during Q&P processing [3]. Structural strengthening (σ_{HP}) can be estimated using the Hall–Petch equation [14, 16, 17]:

$$\sigma_{HP} = K_{HP}D^{-0.5}, \quad (4)$$

where K_{HP} is the Hall–Petch coefficient. For this calculation we used K_{HP} = 160 MPa μm$^{0.5}$, obtained for

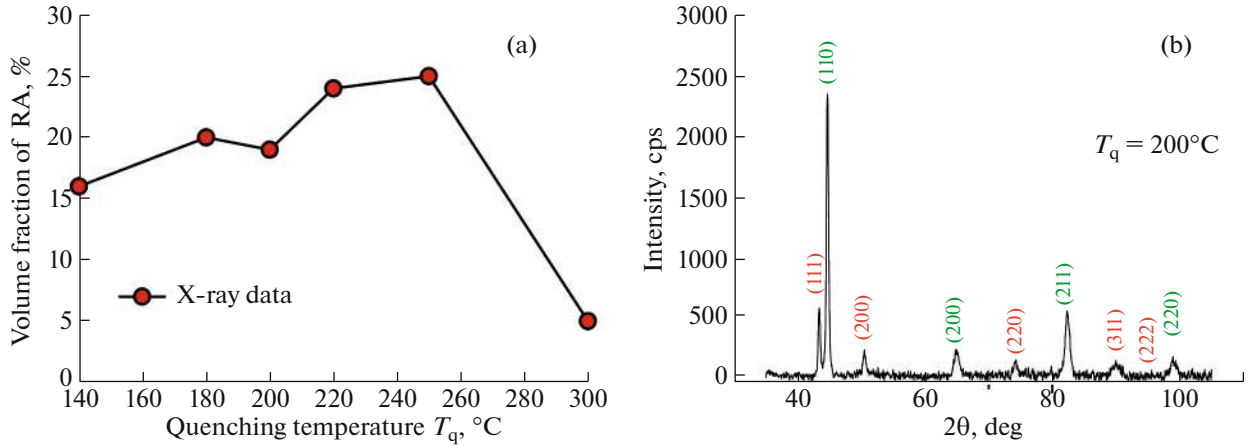

Fig. 3. (a) Effect of quenching temperature on the volume fraction of RA; (b) typical XRD spectrum after quenching at 200°C.

austenitic steel in [14]. Dislocation strengthening (σ_{disl}) can be expressed by the Taylor dependence [14, 16, 17]:

$$\sigma_{disl} = \alpha MGb\rho^{0.5}, \quad (5)$$

where α is the dislocation strengthening coefficient (about 0.24 for materials with an fcc lattice [16]), M is the Taylor coefficient = 3.06 obtained by calculation from misorientation maps, G is the shear modulus (= 75 GPa [17]), b is the Burgers vector (= 0.25 nm), and ρ is the dislocation density, which at $T_q = 200$°C is $\rho = 6.2 \times 10^{14}$ m^{-2}.

According to the calculation according to Eq. (2), $\sigma_{0.2}$ for steel after Q&P at 200°C is $\sigma_{0.2} = 63.5 + 536.5 + 98.3 + 343.4 = 1041.7$ MPa, which coincides with the experimental value of $\sigma_{0.2} = 1120$ MPa with high accuracy.

Consequently, the enrichment of retained austenite with carbon during the "partitioning" operation and the high dislocation density in retained austenite play a major role in achieving high values of $\sigma_{0.2}$ in medium carbon Q&P steel. There is every reason to believe that plastic deformation in the multiphase structure, which is formed in Fe-0.44%C steel after Q&P treatment, begins in the least strong phase, which is retained austenite. Q&P treatment provides high strength of retained austenite, which is the reason for the high yield strength of medium-carbon Q&P steels with a large specific volume of this phase with a block morphology.

Thus, Fe-0.44%C steel after Q&P treatment has high values of the parameter $\sigma_B \delta > 30$ GPa %, and yield strength $\sigma_{0.2} > 1000$ MPa. This is due to the high-volume fraction of retained austenite ~25%, which has a block morphology, high carbon content (~1.3%), and high density of lattice dislocations (~6×10^{14} m^{-2}). The morphology of retained austenite causes the majority of it to transform into martensite during tension (TRIP effect), which provides a high value of strain hardening, and this, in turn, allows one to achieve high values of ultimate strength and relative elongation at the same time. A combination of high strength and ductility can be obtained in Q&P steels with a high content of retained austenite if this phase, in addition to the ability to transform into deformation martensite, has high strength due to the high carbon content and high dislocation density.

ACKNOWLEDGMENTS

The studies were carried out on the equipment of the Joint Scientific Center for Technologies and Materials of Belgorod State National Research University.

FUNDING

This research was funded by the Ministry of Science and Higher Education of the Russian Federation, grant no. 075-15-2021-572.

CONFLICT OF INTEREST

The authors of this work declare that they have no conflicts of interest.

REFERENCES

1. N. Fonstein, *Advanced High Strength Sheet Steels* (Springer Int., Cham, 2015).
2. Zh. Xiong, P. J. Jacques, A. Perlade, and Th. Pardoen, Metall. Mater. Trans. A **50**, 3502 (2019). https://doi.org/10.1007/s11661-019-05265-2
3. J. Speer, D. K. Matlock, B. C. de Cooman, and J. G. Schroth, Acta Mater. **51**, 2611 (2003). https://doi.org/10.1016/S1359-6454(03)00059-4
4. J. Zhao and Z. J. Jiang, Prog. Mater. Sci. **94**, 174 (2018). https://doi.org/10.1016/j.pmatsci.2018.01.006

5. E. J. Seo, L. Cho, Yu. Estrin, and Br. C. de Cooman, Acta Mater. **113**, 124 (2016). https://doi.org/10.1016/j.actamat.2016.04.048
6. K. Zhang, P. Liu, W. Li, Zh. Guo, and Y. Rong, Mater. Sci. Eng. A **619**, 205 (2014). https://doi.org/10.1016/j.msea.2014.09.100
7. B. An, C. Zhang, G. Gao, X. Gui, Z. Tan, R. D. K. Misra, and Z. Yang, Mater. Sci. Eng. A **757**, 117 (2019). https://doi.org/10.1016/j.msea.2019.04.099
8. S. V. Rushchits, A. M. Akhmed'yanov, A. N. Makovetskii, and A. O. Krasnotalov, Vestn. YuUrGU **18** (4), 89 (2018). https://doi.org/10.14529/met180410
9. M. Soleimani, A. Kalhor, and H. Mirzadeh, Mater. Sci. Eng. A **795**, 140023 (2020). https://doi.org/10.1016/j.msea.2020.140023
10. X. C. Xiong, B. Chen, M. X. Huang, J. F. Wang, and L. Wang, Scr. Mater. **68**, 321 (2013). https://doi.org/10.1016/j.scriptamat.2012.11.003
11. A. Zhilyaev, I. Shakhova, A. Belyakov, R. Kaibyshev, and G. Langdon Terence, Wear **305**, 89 (2013). https://doi.org/10.1016/j.wear.2013.06.001
12. K. Chen, Z. Jiang, F. Liu, H. Li, C. Kang, W. Zhang, and A. Wang, Metall. Mater. Trans. A **51**, 3565 (2020). https://doi.org/10.1007/s11661-020-05777-2
13. H. Kitahara, R. Ueji, N. Tsuji, and Y. Minamino, Acta Mater. **54**, 1279 (2006). https://doi.org/10.1016/j.actamat.2005.11.001
14. M. Odnobokova, A. Belyakov, N. Enikeev, R. Kaibyshev, and R. Z. Valiev, Metals **10**, 1614 (2020). https://doi.org/10.3390/met10121614
15. V. G. Gavriljuk and H. Berns, *High Nitrogen Steels: Structure, Properties, Manufacture* (Springer, Berlin, 1999), Application B.
16. S. Malopheyev, V. Kulitskiy, and R. Kaibyshev, J. Alloys Compd. **698**, 957 (2017). https://doi.org/10.1016/j.jallcom.2016.12.289
17. M. V. Odnobokova, A. N. Belyakov, P. D. Dolzhenko, M. V. Kostina, and R. O. Kaibyshev, Mater. Lett. **331**, 133502 (2023). https://doi.org/10.1016/j.matlet.2022.133502